RSC Advances

RSC Advances

www.rsc.org/advances

ROYAL SOCIETY OF CHEMISTRY

www.rsc.org/advances

1   **Thermochemical recovery technology for improved modern engine fuel economy - Part 1: Analysis of**
2   **a prototype exhaust gas fuel reformer**

3   D. Fennell [a], J. Herreros [a], A. Tsolakis [a], K. Cockle [b], J. Pignon [b], P. Millington [b]

4   [a] School of Mechanical Engineering, University of Birmingham, Edgbaston, Birmingham, B15 2TT
5   [b] Johnson Matthey Technology Centre, Blount's Court, Sonning Common, Reading, RG4 9NH
6   * Corresponding author: a.tsolakis@bham.ac.uk
7   Tel: +44 121 414 4170

8
9
10   **Abstract**

11   Exhaust Gas Fuel Reforming has the potential to improve the thermal efficiency of internal combustion

12   engines, as well as simultaneously reduce gaseous and particulate emissions. This thermochemical

13   energy recovery technique aims to reclaim exhaust energy from the high temperature engine exhaust

14   stream to drive catalytic endothermic fuel reforming reactions; these convert hydrocarbon fuel to

15   hydrogen-rich reformate. The reformate is recycled back to the engine as Reformed Exhaust Gas

16   Recirculation (REGR), which provides a source of hydrogen to enhance the engine combustion process

17   and enable high levels of charge dilution; this process is especially promising for modern gasoline direct

18   injection (GDI) engines.

19   This paper presents a full-scale prototype gasoline reformer integrated with a multi-cylinder GDI

20   engine. Performance is assessed in terms of the reformate composition, the temperature distribution

21   across the catalyst, the reforming process (fuel conversion) efficiency and the amount of exhaust heat

22   recovery achieved.

23   **Keywords**
24   Exhaust-gas fuel reforming; hydrogen; reformate; Reformed Exhaust Gas Recirculation (REGR); energy
25   recovery

26   **Abbreviations**
27   TDC   Top Dead Centre
28   CO   Carbon Monoxide
29   EGR   Exhaust Gas Recirculation
30   EGT   Exhaust Gas Temperature
31   FTIR   Fourier transform infra-red detector
32   GC-FID   Gas chromatograph with flame ionisation detector
33   GC-TCD   Gas chromatograph with thermal conductivity detector
34   GDI   Gasoline Direct Injection
35   GHSV   Gas hourly space velocity
36   HC   Hydrocarbon
37   IMEP   Indicated Mean Effective Pressure
38   LHV   Lower heating value
39   NO_x Oxides of Nitrogen
40   PM   Particulate Matter
41   REGR   Reformed Exhaust Gas Recirculation
42   TWC   Three Way Catalyst

43   WGS   Water-gas shift reaction

1. Introduction

45   Exhaust gas fuel reforming is a technique with potential to achieve energy recovery from the exhaust

46   stream of internal combustion engines in order to raise the engine thermal efficiency and reduce fuel

47   consumption, as well as reduce exhaust emissions [1-3]. The feasibility of this thermochemical energy

48   recovery process relies on ensuring that the overall process is endothermic and energy is captured from

49   the exhaust stream. The major reforming reactions are listed in Table 1. The two primary chemical

50   reactions, steam reforming (1) and dry reforming (2) are endothermic and reform hydrocarbon (HC)

51   fuel into hydrogen and carbon monoxide with a net gain in fuel enthalpy. Carbon dioxide and steam are

52   supplied as reactants by the engine exhaust gas, and the hydrogen-rich product gases are re-circulated

53   to the intake system for in-cylinder combustion, completing the reformed exhaust gas recirculation

54   (REGR) system.

55   If oxygen is present in the exhaust gas then some fuel will be consumed by highly exothermic oxidation

56   reactions. Previous exhaust gas fuel reforming studies [4] have revealed that the combustion reaction (3)

57   prevails but some partial oxidation (4) is also possible. In some applications the oxidation reactions are

58   used to increase the catalyst temperature in order to improve the hydrogen yield, for instance by

59   Partial Oxidation reformers and Autothermal reformers. The less exothermic water-gas shift (WGS)

60   reaction (5) also increases the hydrogen concentration by reacting CO, which has already been

61   produced by the other reforming reactions, with steam. The process efficiency is reduced to some

62   degree by these exothermic reactions.

63   Table 1 – General formulae for the key reforming reactions in hydrocarbon fuel reforming

Reaction	General chemical formula	* Enthalpy of reaction, MJ/kmol	
Steam reforming:	$C_xH_y + xH_2O \rightarrow xCO + (x + \frac{y}{2})H_2$	$\Delta h_R = (+\ 1259)$	(1)
Dry reforming:	$C_xH_y + xCO_2 \rightarrow 2xCO + \frac{y}{2}H_2$	$\Delta h_R = (+\ 1588)$	(2)
Combustion:	$C_xH_y + (x + \frac{y}{4})O_2 \rightarrow xCO_2 + \frac{y}{2}H_2O$	$\Delta h_R = (-\ 5116)$	(3)
Partial oxidation:	$C_xH_y + \frac{x}{2}O_2 \rightarrow xCO + \frac{y}{2}H_2$	$\Delta h_R = (-\ 676)$	(4)
Water-gas shift:	$CO + H_2O \rightleftharpoons CO_2 + H_2$	$\Delta h_R = (-\ 283)$	(5)

64   * when calculating enthalpy of reaction it was assumed that: HC fuel is *n*-octane; reactions go to completion;
65   products and reactants are at 25°C and 1 atm; and water is in the gaseous state. Thermodynamic data from [5]
66
67   Other classifications of reformer have been researched for on-board hydrogen generation in the past.

68   Partial oxidation reformers [5-7] react air and HC fuel to produce reformate, which, when coupled with a

69   gasoline engine, can extend the (air or EGR) dilution limit and improve engine efficiency and emissions.

70   These systems can be useful for cold engine starts operating partially or solely on reformate in order to

71   reduce emissions during warm-up [6, 7]. However, the engine-reformer system efficiency ultimately

72   suffers due to energy lost in the exothermic partial oxidation reforming process. A plasma reformer [8, 9]

73   instead uses electrical power to convert HC fuels to reformate. Again, the overall engine-reformer

74   system efficiency is reduced due to the electrical power required for the reforming process. None of

75   these systems aim to achieve exhaust heat recovery.

76   Ethanol reformers designed to achieve heat recovery from ethanol-fuelled [10] and gasoline-fuelled [11] SI

77   engines have been developed more recently. Ethanol can be reformed more easily than the longer

78   chain and more complex (e.g. aromatic) HC components of gasoline and so it is possible at lower

79   temperature, typically between 300-350 °C [10]. This makes ethanol reforming feasible over most of the

80   operating range of a SI engine.

81   The gasoline reformer has potential for more widespread use than ethanol and E85 but greater

82   technical barriers to overcome, most notably with respect to achieving effective performance at

83   sufficiently low temperature to be feasible with the gasoline engine exhaust stream. Because reformer

84   performance is heavily dependent upon catalyst temperature, reformer design should be focussed to

85   ensure efficient heat transfer from the exhaust stream and minimise heat loses [4, 12].

86   Exhaust gas fuel reforming has great potential for improving engine efficiency and reducing exhaust

87   emissions. A review article by Golunski [13] discussed the application of exhaust gas fuel reforming for

88   improving the thermal efficiency of IC engines through enhanced combustion and novel after-

89   treatment solutions. Thermodynamic and experimental studies of the REGR reactions have shown that

90   precious metal catalysts, e.g. Rhodium on Zirconia [14, 15], exhibit high activity with yields close to

91   equilibrium at temperatures typical of the gasoline engine exhaust. A recent experimental study [1] using

92   hydrogen and CO addition to conventional EGR highlights the potential benefits that REGR can offer to

93   the GDI engine, with simultaneous reductions in NO_x, PM and CO, only slightly increased HCs, and

94   increased engine and total system thermal efficiency.

95   This paper furthers the research in the field of exhaust gas fuel reforming as, for the first time, a full-

96   scale gasoline reformer integrated with a modern production multi-cylinder GDI engine was studied.

97   The results discussed in this paper are focussed on the prototype reformer performance; this includes

98   examination of the reformer temperature profiles, analysis of the reformate composition including HC

99   speciation, and calculation of the reformer fuel conversion efficiency. Devices designed to achieve

100   exhaust heat recovery may be subjected to exergy analysis, and this has been applied here to establish

101   the influence of exhaust gas fuel reforming on the exergy, or 'available energy', of the exhaust stream.

102   The efficiency and emissions performance of the GDI engine utilising exhaust gas fuel reforming will be

103   presented in a follow-up paper.

104 **2. Experimental setup and test conditions**

105 The reformer and catalyst were designed by Johnson Matthey and it consists of a stack of five metallic

106 catalyst plates (8.8in^3 each) coated with 3.6g/in^3 of ceramic support (Ceria-Zirconia-Alumina) loaded

107 with 3.3% Platinum - 1.7% Rhodium. Rhodium offers very good sulphur tolerance, excellent thermal

108 stability and resistance to coking, and stable catalyst performance was experienced throughout the 6

109 month test program. Each catalyst plate is mounted between two finned stainless steel plates used to

110 seal it from the exhaust stream. The reformer plate assembly was designed to ensure high heat transfer

111 from the hot exhaust gas to the catalyst, using fins on the stainless steel surround for increased surface

112 area and a narrow catalyst construction only four cells thick. The exhaust stream flows over the

113 reformer plate stack, which is positioned after the TWC. The reformer feed gas is extracted from the

114 exhaust stream before the TWC, mixed with gasoline, and routed around the outer skin of the TWC to

115 assist with fuel vaporisation and feed gas pre-heating. The required flow rate of gasoline was injected

116 into the reformer feed gas by varying the pulse-width of a solenoid fuel injector, typically used in port

117 injection engines, operating at a fixed frequency of 30Hz. The injector was mounted to the reformer

118 with a manifold cooled by engine water to protect the injector from high exhaust system temperatures.

119 11 thermocouples were distributed over the middle reformer plate according to schematic Figure 1,

120 with additional thermocouples in the feed gas, product gas, and exhaust stream before and after

121 passing over the reformer assembly.
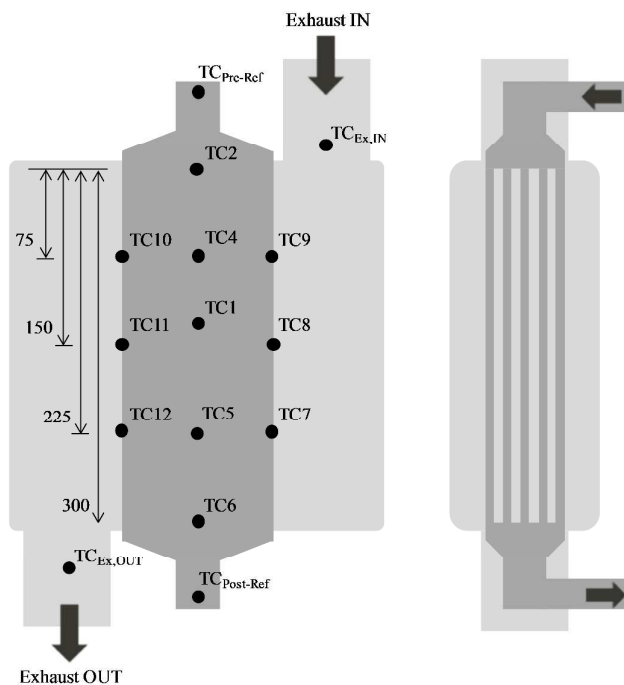
122
123 Figure 1 - Reformer schematic indicating thermocouples (TC) locations on the central reformer plate
124 and in the exhaust stream

4

125   *Reformer installation***:** The reformer was installed with a turbocharged 2L GDI engine, positioned in the

126   exhaust stream after the TWC. The REGR system installation used a 'high pressure' recirculation

127   configuration, inducting reformate directly into the intake manifold. The system consisted of an

128   integrated DC motor controlled EGR valve and cooler, and an additional cooler, all supplied with engine

129   coolant to maintain acceptable gas and component temperatures.

130   *Reformate analysis:* A MKS Instruments Multigas 2030 Fourier Transform Infra-Red (FTIR) spectrometer

131   was used to analyse the reformate stream for multiple species, including CO_2, CO, H_2O, NH_3 and a

132   selection of hydrocarbons compounds including methane. A HP 5890 Series 2 gas chromatograph with

133   thermal conductivity detector (GC-TCD) and HP 3395 integrator was used to measure the hydrogen

134   concentration in the reformate stream. Argon at 40psi acted as the carrier gas to the sample fed at

135   10psi, resulting in the hydrogen peak occurring at 2.4s retention time. The detector was calibrated with

136   10% and 30% hydrogen in nitrogen. Another HP 5890 Series 2 gas chromatograph with flame ionisation

137   detector (GC-FID) gave in-depth speciation of the HC components of the reformate. The GC-FID was

138   calibrated with 15 common HCs ranging from C1 to C7 (Table 2).

139   Table 2 – Hydrocarbon species included in GC-FID calibration

HC species	Formula	HC species	Formula	HC species	Formula
Methane	CH_4	1 - butane	C_4H_{10}	n-pentane	C_5H_{12}
Ethylene	C_2H_4	1,3-Butadiene	C_4H_6	n-hexane	C_6H_{14}
Propylene	C_3H_6	n-butane	C_4H_{10}	Benzene	C_6H_6
Propane	C_3H_8	3-Methyl-1-butene	C_5H_8	n-heptane	C_7H_{16}
Iso-butane	C_4H_{10}	Iso-pentane	C_5H_{12}	Toluene	C_7H_8

140   A Horiba MEXA-7100DEGR measured the intake manifold and exhaust stream CO_2 concentration in

141   order to calculate the charge dilution rate according to equation (6). The FID component of the Horiba

142   analyser was also useful for providing a measurement of the total HC content of the reformate, which

143   was not possible with the FTIR analyser.

$$Charge\ Dilution\ Rate, \% = \frac{(CO_2)_{manifold}}{(CO_2)_{exhaust}} x100 \qquad (6)$$

144   *Test conditions*: Three engine conditions were selected in order to generate a suitable range of

145   reformer temperature and flow conditions; these were 35Nm/3bar IMEP at 2100rpm, 50Nm/4bar IMEP

146   at 3000rpm, and 105Nm/7.2bar IMEP at 2100rpm. The first two conditions are key steady state

147   conditions used on the new European drive cycle for a mid-size/large family vehicle with a 2 litre

148   engine, and the third condition is typical of a higher load transient condition. At each condition the

149   engine was operated with the maximum achievable charge dilution rate, and also a lower dilution rate

150   to investigate the effect of reformer mass flow rate, or gas hourly space velocity (GHSV). Gasoline was

151   injected into the reformer feed gas such that the molar concentration was 0.5% and 1% (fuel

152   composition assumed to be octane) to test the influence of fuel concentration on reformer

153   performance. Excess fuel can result in a reversible catalyst deactivation by coke lay down. The fuel

154   addition was optimised to avoid this fouling while maintaining good H_2 production and the test

155   procedure involved periodically operating with EGR to expose the catalyst to steam and oxygen in order

156   to reverse any coking that may have occurred.

157   The engine-out exhaust gas composition (Table 3) varied little across the range of conditions tested

158   because the engine uses a homogeneous, stoichiometric combustion strategy. This can also be

159   considered the reformer feed gas composition (prior to gasoline injection). The slight variations of the

160   primary exhaust gas species at each engine condition are due to the use of different charge dilution

161   rates which influenced the combustion. This also results in larger percentage variation of NO_x and THCs

162   due to the effects of REGR on the combustion process. The oxygen content of the exhaust stream varies

163   only between 0.5 to 0.7%, which is of particular relevance to the reformer process efficiency as the

164   oxygen concentration is directly proportional to the amount of fuel that is oxidised in the reformer and

165   the resulting increase in temperature.

166   Table 3 - Exhaust gas temperature (EGT) and composition at each engine condition

Engine condition	EGT, °C (Pre-reformer)	CO_2, %	O_2, %	CO, %	* H_2O, %	NO_X, ppm	THC, ppm
35Nm/ 2100rpm	595 - 605	14.8 - 15.0	0.60 - 0.70	0.50 - 0.60	14.3- 14.4	100 - 1200	1900 - 3000
50Nm/ 3000rpm	655 - 680	14.8 - 14.9	0.50 - 0.65	0.50 - 0.55	14.3- 14.4	200 - 600	1500 - 1900
105Nm/ 2100rpm	685 - 720	14.8 - 15.0	0.60 - 0.65	0.55 - 0.70	14.4- 14.5	900 - 2300	1300 - 1600

* Calculated

167   **3. Results and discussion**

168   **3.1. Reformate characteristics**

169   *Temperature distribution:* The temperature distribution across the middle reformer plate varies with

170   engine condition, REGR flow rate, fuel concentration, and the resulting reforming activity (Figure 2). In

171   these plots the reformer feed gas flows from top to bottom and the engine exhaust stream flows over

172   the plate from right to left. The temperatures were generally higher along the right edge due to the

173   exhaust stream heating. The baseline plots clearly show that the reformer plates are more effectively

174   heated as the exhaust stream temperature increases with engine load.

175   At the lowest temperature condition (35Nm/2100rpm) the plate temperatures drop as the REGR flow is

176   increased up to 20% due to reforming activity. There is also a slight cooling effect just by flowing gas

177   through the reformer (i.e. with EGR), analogous to a forced-convection cooling process. At the highest

178   REGR flow rate there is a slight increase in reformer temperature with a more even distribution. This is

179   the result of multiple effects associated with increasing the flow rate: more oxygen is available for fuel

180   oxidation which increases the gas temperature in the front of the reformer; the high flow rate moves

181   the high temperature gas along the reformer more quickly resulting in the more even distribution; and

182   reforming activity tends to be lower as the flow rate increases.

183   At the two higher engine load conditions the reformer is heated to significantly higher temperature

184   when there is no REGR flow (baseline condition). Increasing either the REGR flow or the fuel

185   concentation lowers the reformer temperature. Both of these changes increase the availability of fuel

186   while, importantly, at sufficiently high temperature for the endothermic reforming reactions to be

187   feasible. Again, increasing the REGR flow rate results in a more even temperature distribution.

188

189

190
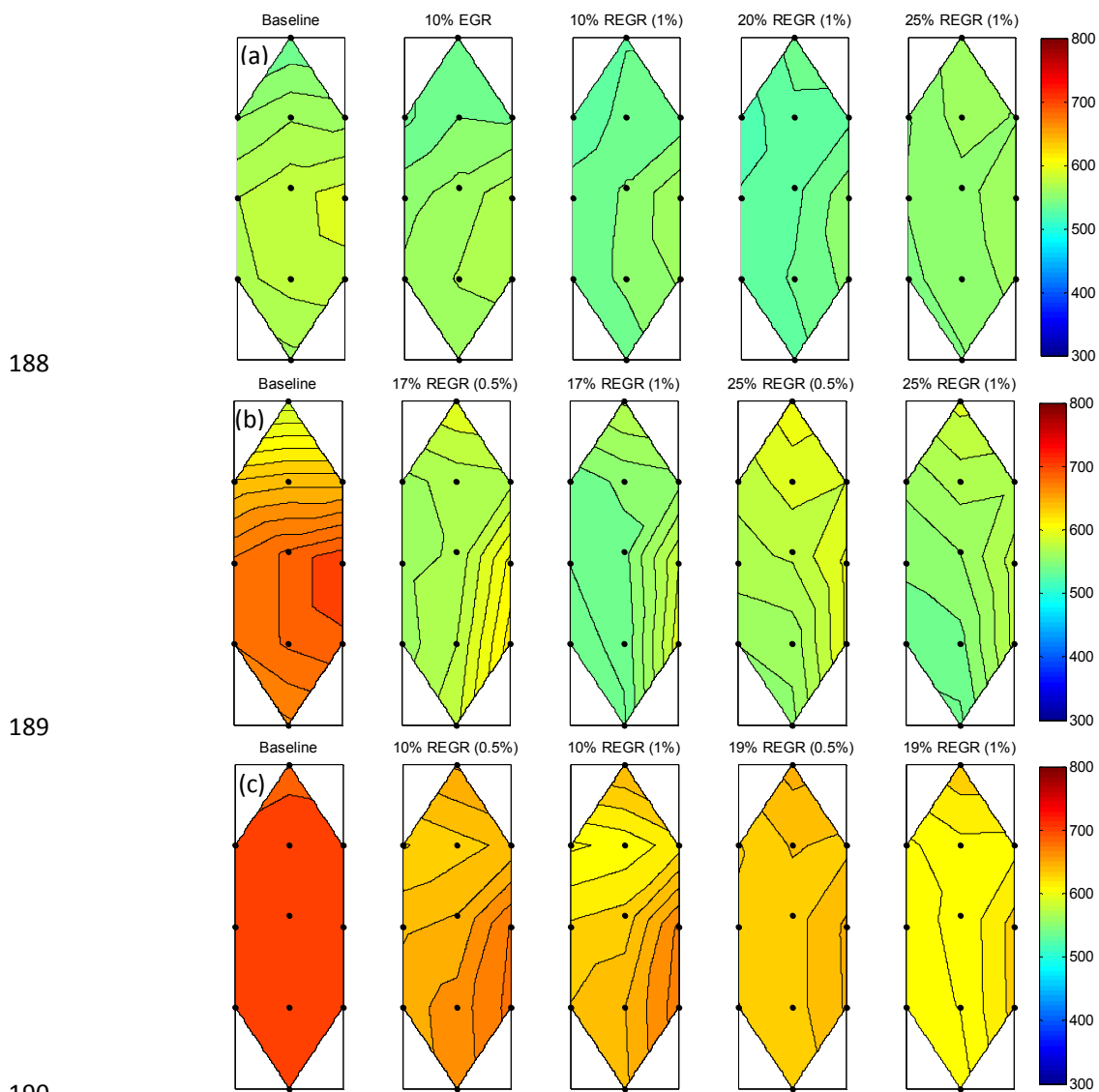
191   Figure 2 – Temperature (°C) distribution across the middle reformer plate at a) 35Nm, b) 50Nm and c)
192   105Nm engine conditions, for a range of REGR concentrations (vol.) in the intake charge with either
193   0.5% or 1% (vol.) gasoline in the reformer feed gas

194

195   *Linear reformer temperature profiles:* Figure 3 compares the linear reformer temperature profiles while

196   reforming with two different mass flows, 4.5 and 14.5kg/h - this equates to 10% and 25% REGR in terms

197   of the dilution rate at the 35Nm/2100rpm engine condition. Temperature profiles are included for 0.5%

198   and 1% fuel in the reformer feed gas. At low reactant mass flow rate in the reformer, there was very

199   little heating due to exothermic reactions in the front of the catalyst. There was no indication of

200   endothermic reforming cooling the reformer. It appears that a small amount of reforming occurred in

201   the first 75mm of the reformer as the temperature remains approximately constant. After this the

202   temperature increased due to heating by the main engine exhaust stream. At the higher reactant flow

203   rate there was a greater quantity of fuel and oxygen passing through the reformer which led to a larger

204   temperature increase at the front face. The combination of higher temperature and more fuel being

205   available for reforming meant that there was a clear drop in temperature along the length of the

206   reformer due to endothermic reforming reactions.
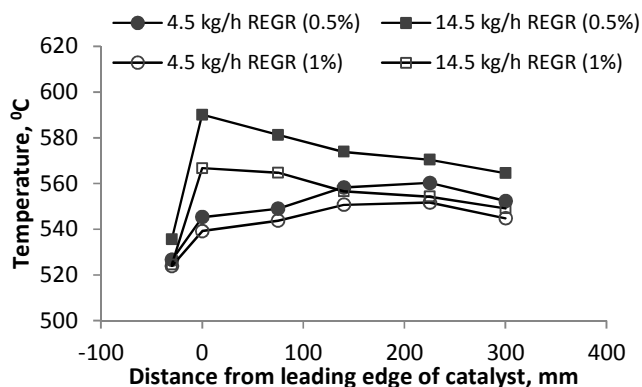
207
208   Figure 3 – Linear reformer temperature profile at the low temperature (35Nm/2100rpm) condition.

209   Increasing the fuel concentration in the feed gas (for a given reactant flow rate) results in a reasonably

210   uniform reduction of the temperature along the reformer. The feed gas temperature (-30mm from

211   leading edge) was slightly lower for the higher fuel flow conditions due to greater cooling by fuel

212   vaporisation, and the gradient of the rise in temperature between the feed gas (-30mm) and the

213   leading edge (0mm) was similar when comparing each fuel concentration condition. The amount of

214   oxygen available for oxidation is dependent on the reactant flow rate and determines the amount of

215   heating at leading edge. The slight reduction of heating with increasing fuel concentration is likely due

216   to the higher rate of endothermic reforming (decrease in the oxygen/carbon ratio) and slightly higher

217   specific heat capacity of the feed gas.

218   The effect of reactant mass flow rate in the reformer on the linear temperature profile is shown in

219   Figure 4 for two engine loads with 1% feed gas fuel concentration in each case. This shows the location

220   of endothermic reforming moving further along the reformer with increasing flow rate. The initial drop

221   in temperature is greater for the lower flow condition at each load.

8

222   When the reformer flow is low and the reformer plate temperature is relatively high at the inlet, 650°C

223   at the 105Nm condition, most of the reforming occurs in the first section of the reformer and is

224   followed by re-heating. This implies that the reformer is able to process more fuel than is being

225   supplied at the low flow condition.
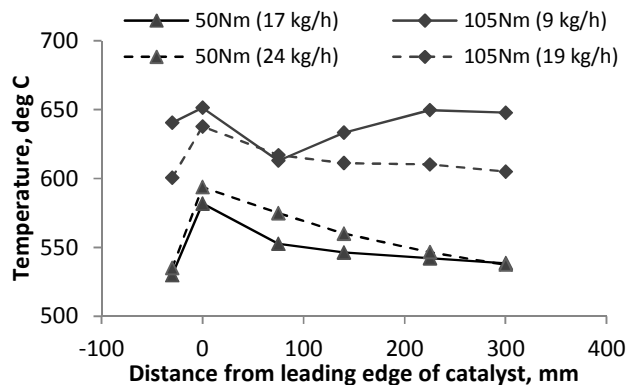
226
227   Figure 4 - Linear reformer plate temperature profiles for high and low REGR flows at two engine
228   conditions (1% feed gas fuel concentration in each case)

229   Comparing the two curves for the high temperature condition (105Nm) there is a large temperature

230   difference in the final 100mm of the reformer. The conditions in this section can be used to give an

231   insight into the equilibrium position of the WGS reaction. The reformer temperature is reduced for the

232   higher REGR rate which increases the WGS reaction equilibrium constant, resulting in an equilibrium

233   shift towards higher H_2 and CO_2 concentration by consuming CO and H_2O. For this reason, increasing

234   the REGR rate generally results in a greater hydrogen/CO ratio (providing conditions are reasonable for

235   reforming) this can be seen by comparing the hydrogen and CO data in Figure 55, particularly for the 1%

236   feed gas fuel concentration conditions.

237   It should be emphasised that the linear profiles offer a 1-dimensional view of the reformer operating

238   temperature. This information disregards the temperature distribution across each reformer plate and

239   any difference between the five individual plates.

240   *Reformate speciation:* Maximum hydrogen production was observed when the consumption of steam

241   was greatest, which indicates successful promotion of the steam reforming reaction (Fig. 5). This

242   occurred at the 50Nm/3000rpm engine condition, when there was 11% hydrogen produced and 6% un-

243   reacted steam measured in the reformate, and there was a combination of high temperature and

244   intermediate reactant flow rate. Some CO_2 can be expected to be produced by oxidation and WGS

245   reactions, and may be consumed by the dry reforming reaction.   The CO_2 concentration in the

246   reformate was relatively consistent at most test points but was reduced slightly for low REGR mass flow

247   rates. It should be noted that for a given engine load, at lower REGR mass flows the reformer plate

248   temperatures are higher. This means the reversible WGS reaction has a smaller equilibrium constant, is

249   therefore less favourable towards the reaction products, and so less hydrogen and CO_2 are produced by
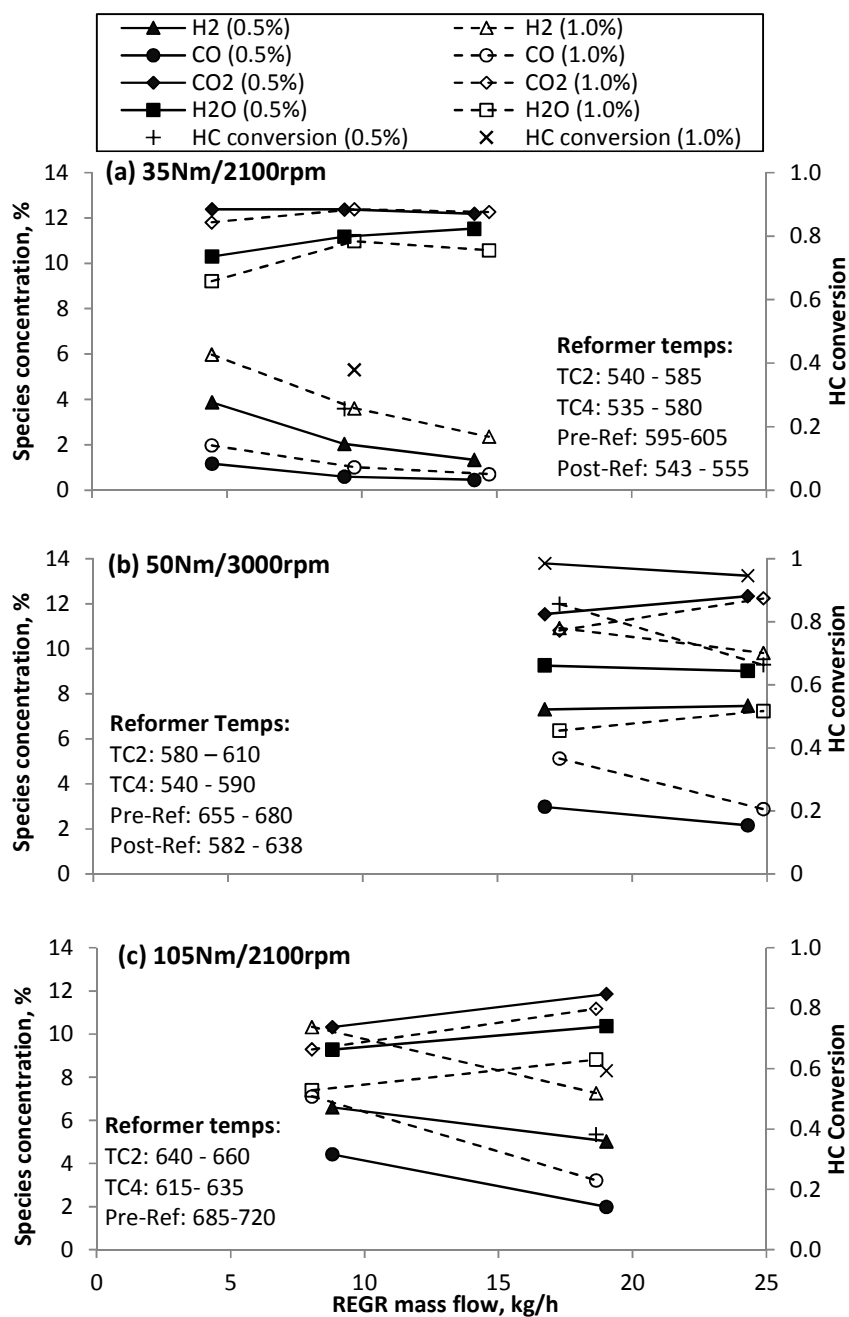
250   this reaction.

Figure 5 - Reformate species concentrations at various engine conditions (a) 35Nm, (b) 50Nm and (c) 105Nm

251

252   *Hydrocarbon speciation:* The proportion of HCs that breakthrough the reformer increases with REGR

253   flow rate; therefore at 17kg/h REGR (Figure 6a) there is a lower total HC (THC) concentration. The

254   calibration gas used contains many of the major components (Table 2) of gasoline and there were no

255   significant peaks in the chromatogram spectrum unaccounted for.

256   Methane made up a greater proportion of the HCs in the reformate at lower REGR flow, partly because

257   the total breakthrough HC quantity was lower, but also due to higher methane production by the

11

258   'methanation' reforming side reactions; these consume hydrogen in reactions with CO, CO_2 or HCs to

259   produce methane, but tend to be relatively unfavoured under REGR conditions [14]. The higher

260   concentration of H_2 and CO produced by the primary reforming reactions at lower REGR flow will lead

261   to the methanation reactions being increasingly favoured.

262   The molar composition of the gasoline was 12.6% paraffins, 33.4% isoparaffins, 14.6% olefins, 5.1%

263   naphthenes, 28.9% aromatics and 4.9% oxygenates. The measured aromatic fraction (benzene +

264   toluene) was higher in each case at 37% and 51%. This supports the idea that the aromatic fraction of

265   the gasoline is not being reformed as readily as the less complex HCs such as the paraffins, which

266   constitute nearly half of the gasoline mixture and appear in significantly lower quantity in the

267   reformate. There is also a smaller toluene/benzene ratio at low reactant flow which implies toluene is

268   reformed more readily than benzene. It may be that some toluene is partially reformed to the more

269   stable/less reactive benzene.
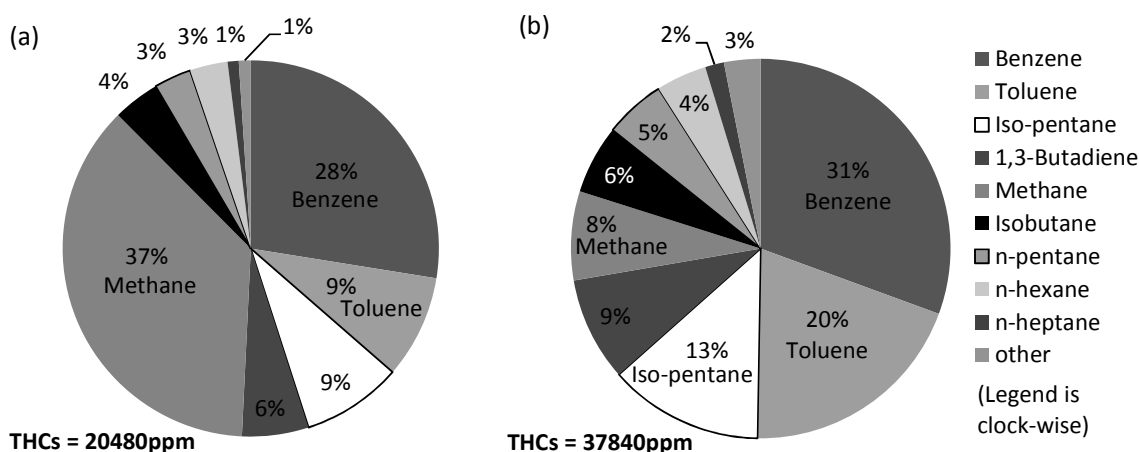
270   Figure 6 - Proportion of HC species of the total HCs in reformate as measured by GC-FID at
271   50Nm/3000rpm with REGR (1% fuel): 17 kg/h (a) and 24 kg/h (b)

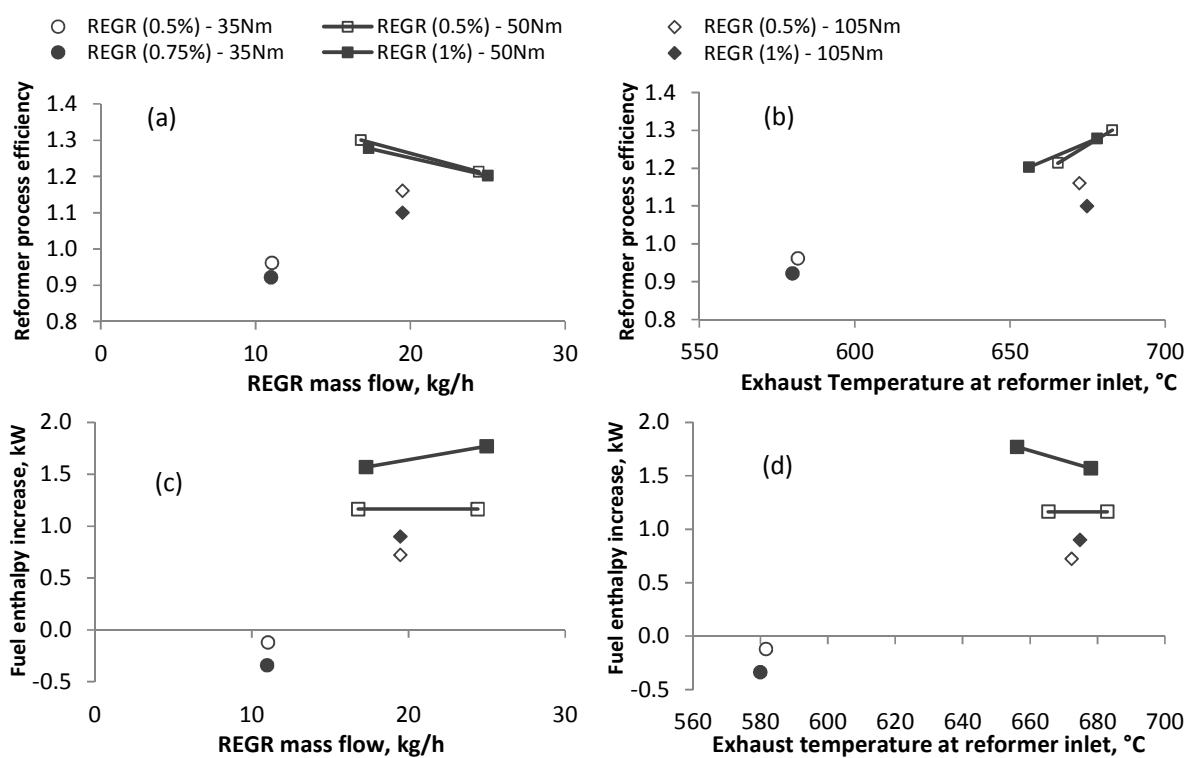### 3.2 Reformer process efficiency

273   The effectiveness of the reformer can be analysed by calculating the reformer process efficiency using

274   Equation (7). In this equation the HCs and CO contained in the engine exhaust gas which is fed in the

275   reformer are not included in the calculation of the reformer efficiency. However, they are supplied to

276   the reformer as products of incomplete in-cylinder combustion, and would usually be considered

277   wasted energy as the exhaust heat, being both uncombusted species and exhaust heat being used in

278   the reformer. Therefore equation 7 calculates reformer process efficiency without including those

279   species as an input energy, contributing in the increase of the reforming process efficiency (Figure 7).

280   'Dry' measurements were converted to 'wet' molar fractions (using knowledge of the steam

281   concentration in the feed gas/reformate) before calculating the mass flow rate of individual species.

$$Reformer\ process\ efficiency, \eta_{ref} = \frac{LHV_{H2}.\dot{m}_{H2} + LHV_{CO}.\dot{m}_{CO} + LHV_{CH4}.\dot{m}_{CH4} + LHV_g.\dot{m}_{HC,out}}{LHV_g.\dot{m}_{g,in}} \qquad (7)$$

282

283   At the two highest engine load conditions, when exhaust temperature is above 650°C, the reformer

284   process efficiency is greater than one (Figure 7a and b). This means that the overall reforming reaction

285   is an endothermic process leading in the increase of the total fuel enthalpy (Figure 7c and d). The

286   reformer process efficiency is similar when comparing fuel concentration at each test point; increasing

287   the fuel concentration to 1% improves further the fuel enthalpy. At the low temperature condition the

288   reformer process efficiency is less than 1, meaning some energy is lost during the gasoline reforming

289   process.

290

291   Figure 7 - Reformer process efficiency (a & b) and Fuel enthalpy increase (c & d) plotted against REGR
292   mass flow (a & c) and exhaust temperature at the reformer inlet (b & d)

293   **3.3 Exhaust energy recovery**

294   *First law analysis - Exhaust stream energy:* Under normal engine operating conditions, i.e. when there is

295   no reforming, the exhaust stream temperature drops (by some amount ΔT) as it passes across the

296   reformer due to heat loss to the atmosphere. This is perhaps an obvious statement; however it is

297   necessary to consider this heat loss when estimating the amount of exhaust energy recovery achieved

298   by the reformer. When operating with EGR or REGR at a given engine load and recirculation rate, the

299   exhaust stream mass flow, composition, and temperature at the reformer inlet are very similar;

300   therefore it may be assumed that the heat loss to atmosphere is the same under each condition.

301   When the reformer is switched on there will be a greater exhaust stream temperature differential

302   (ΔT_{REGR}) if energy is extracted by the overall endothermic reforming process. This means that the

303   exhaust stream temperature drop due to reforming, ΔT_{Ref} can be estimated for each condition using

304    $\Delta T_{Ref} = \Delta T_{REGR} - \Delta T_{EGR}$. The rate of exhaust heat recovery is then approximately equal to the change in

305   enthalpy of the exhaust gases as they drop in temperature by ΔT_{Ref}, and is calculated using equation (7).

306   The specific heat capacity of the exhaust stream, c_{exh}, was calculated for the mixture of nitrogen, CO_2

307   and steam (post-TWC composition) at the average of the pre- and post-reformer exhaust stream

308   temperature.

$$\textbf{Exhaust heat recovery,} \quad \dot{Q} = \dot{H} = \dot{m}_{exh} \cdot \bar{c}_{p,exh} \cdot \Delta T_{Ref} \quad \text{(kW)} \quad (7)$$

309   The rate of exhaust stream heat recovery achieved by fuel reforming at each engine condition is plotted

310   in Figure 8. The highest rate of heat recovery was achieved at the 105Nm engine condition when the

311   reformer temperature was highest. This engine condition uses intermediate REGR mass flow rates and

312   so the reformer's ability to recover exhaust energy is not compromised by high GHSV. At the 50Nm

313   engine condition, increasing the REGR flow to the highest rate reduces heat recovery due to the

314   combined effects of increased GHSV and lower exhaust stream temperature (increased charge dilution

315   causes lower combustion and exhaust temperatures). In general, increasing the reformer fuel flow

316   increases the amount of exhaust heat recovery.
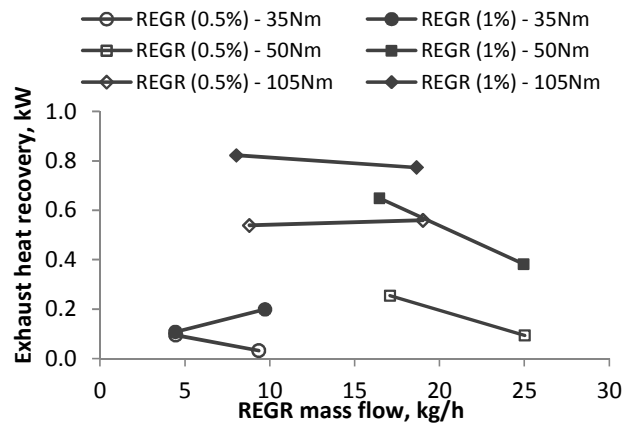
317
318   Figure 8 - Rate of exhaust stream heat recovery with fuel reforming

319   While considering the heat recovery in absolute terms is interesting, it is also important to put these

320   values into perspective; Figure 9 presents the heat recovery as a fraction of the total fuel energy,

321   engine effective work and pre-reformer exhaust stream energy. When working close to optimally at the

322   50Nm and 105Nm conditions, the reformer is able to extract energy from the exhaust stream to

323   recover around 1% of the total fuel energy supplied to the engine and reformer, which equates to

324   between 3-4% of the effective engine work.
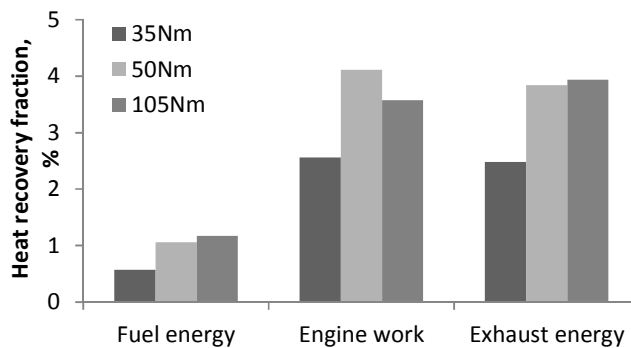
325
326   Figure 9 - Exhaust stream heat recovery as a fraction of total fuel energy, engine effective work and pre-
327   reformer exhaust energy

328   *Second law analysis - Exhaust stream exergy:* According to the second law of thermodynamics, exergy

329   represents the maximum amount of energy that can be extracted by bringing a system at temperature

330   T to the ambient temperature T_0. The exergy of a fluid stream can be evaluated using equation (8) [16].

331   This considers the exergy of the enthalpy, kinetic energy and potential energy of the fluid stream. This

332   analysis was applied to the exhaust stream, which contains multiple gas species, using equation (9) to

333   calculate the 'energy availability' of the pre- and post-reformer exhaust gas, where $\dot{N}_{exh}$ is the molar

334   flow of the exhaust stream (kmol/s) and n_i is the molar fraction of gas species *i*. In this case, T_0 was

335   taken as 298K.

$$\psi = (h - h_0) - T_0(s - s_0) + \frac{V^2}{2} + gz \tag{8}$$

$$\psi_{exh} = \sum \dot{N}_{exh} \cdot n_i \cdot \left[(h_i - h_{i,0}) - T_0 (s_i - s_{i,0}) \right] \qquad \text{(kW)} \tag{9}$$

336   There were various assumptions made during the calculation of exhaust exergy. These included: the

337   exhaust stream is a mixture of ideal gases; specific heat values are taken at the average process

338   temperature, and were calculated using 3rd order polynomial relationships from [16]; the TWC catalyst

339   converts the exhaust stream to a mixture of inert gases (nitrogen, carbon dioxide and steam) with 100%

340   efficiency and therefore the exhaust contains no species with chemical potential energy; the exergy of

341   the kinetic and gravitational potential energy components of the exhaust stream are negligible.

342   As the reformer is designed to recover energy from the exhaust stream, there should be a reduction in

343   exergy, or available energy, across the reformer. A more efficient overall engine-reformer system

344   should also result in a reduction of the exhaust stream exergy (for a given load) at the reformer inlet.

345   This accounts for the influence of REGR on the engine and combustion efficiency, which directly

346   influences the exhaust exergy.

347   Figure 1Figure 10 plots the pre- and post-reformer exhaust stream exergy, as a percentage of the

348   engine brake power, for each test condition at each engine load. These plots show the general trend for

349   reducing exhaust stream exergy with increasing dilution rate and reformed fuel fraction. In each case

350   the baseline condition exhaust exergy is highest; both EGR and REGR reduce the exhaust exergy. The

351 50Nm engine condition represents the highest 'relative' exergy with 60% of the brake power available

352 for recovery; the highest absolute exergy was at the 105Nm condition.

353

354

355
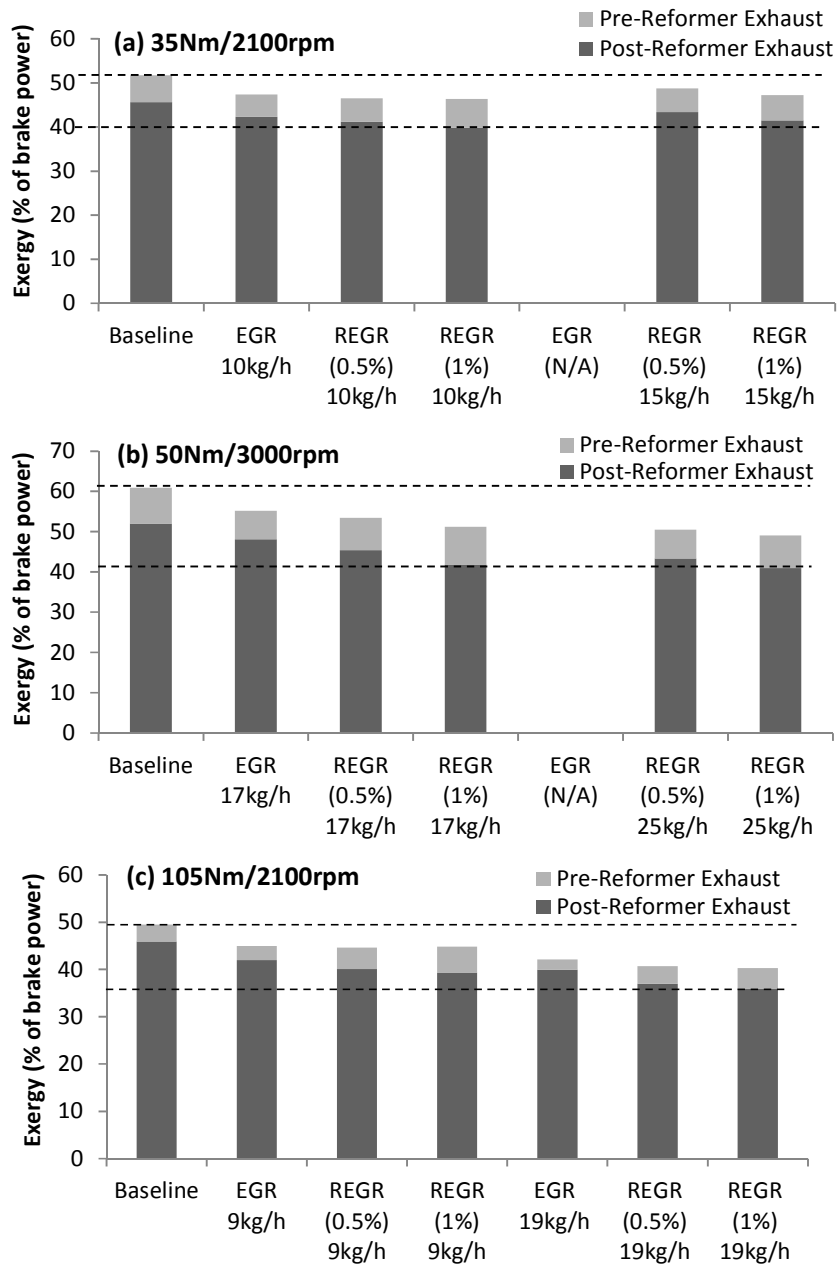
356 Figure 10 - Comparing pre- and post-reformer exhaust stream exergy for a variety of engine conditions
357 (a) 35Nm, (b) 50Nm and (c) 105Nm

358 **4. Conclusions**

359 A full-scale prototype exhaust gas fuel reformer has been coupled with a multi-cylinder GDI engine, and

360 demonstrates that gasoline reforming is feasible as a thermochemical energy recovery technique at

361 typical GDI engine exhaust temperature.

362　At higher exhaust temperatures, the reformer is capable of converting gasoline to hydrogen-rich gas in

363　an overall endothermic process while recovering some exhaust energy. Performance is borderline

364　effective at lower exhaust temperature (for engine conditions representing low vehicle speed); this

365　means that some reforming is possible which produces hydrogen that is beneficial to engine operation,

366　but a small amount of fuel energy is lost in the reforming process.

367　Speciation of reformate produced by the reformer at a range of engine conditions indicates a large

368　variation in reformate quality, with a strong dependence on process temperature and reactant

369　composition.

370　The outlook for fuel reforming may be improved should the trend for engine downsizing continue. By

371　placing a higher demand on the engine by downsizing, there is a shift to higher engine IMEPs for a given

372　road load and the mean exhaust temperature will be increased as a result. It can be concluded from this

373　study is that sustained (medium) engine loads, as used for motorway/highway driving, generate

374　conditions that favour fuel reforming; ultimately this means that exhaust energy recovery can be

375　achieved. The bias of many drive cycles to low engine speed/load conditions, and a high proportion of

376　warm-up time, mean that the fuel reformer is not likely show its full potential 'on cycle' but should

377　offer greater benefits for higher load and sustained driving conditions.

378　**Acknowledgments**

386

387　**References**

388　1.　D. Fennell, J. M. Herreros and A. Tsolakis, *Int J Hydrogen Energ*, 2014, **39**, 5153–5162.

389　2.　P. Leung, A. Tsolakis, J. Rodriguez-Fernandez and S. Golunski, *Energy Environ. Sci.*, 2010, **3**, 780-
390　788.

391　3.　Y. Jamal, T. Wagner and M. L. Wyszynski, *Int J Hydrogen Energ*, 1996, **21**, pp.507 - 519.

392　4.　S. Peucheret, M. Feaviour and S. Golunski, *Appl Catal B-Environ*, 2006, **65**, 201-206.

393　5.　A. A. Quader, J. E. Kirwan and M. J. Grieve, *SAE Paper*, 2003, 2003-01-1356.

394　6.　K. D. Isherwood, J. R. Linna and P. J. Loftus, *SAE Paper*, 1998, 980939.

395　7.　J. E. Kirwan, A. A. Quader and M. J. Grieve, *SAE Paper*, 2002, 2002-01-1011.

396　8.　J. B. Green Jr., N. Domingo, J. M. E. Storey, R. M. Wagner, J. S. Armfield, L. Bromberg, D. R.
397　Cohn, A. Rabinovich and N. Alexeev, *SAE Paper*, 2000, 2000-01-2206.

398　9.　E. J. Tully and J. B. Heywood, *SAE Paper*, 2003, 2003-01-0630.

399   10.   E. D. Sall, D. A. Morgenstern, J. P. Fornango, J. W. Taylor, N. Chomic and J. Wheeler, *Energ Fuel*,
400   2013, **27**, 5579-5588.
401   11.   C. Ji, X. Dai, B. Ju, S. Wang, B. Zhang, C. Liang and X. Liu, *Int J Hydrogen Energ*, 2012, **37**, 7860-
402   7868.
403   12.   C. H. Bartholomew, *Appl Catal A-Gen*, 2001, **212**, 17-60.
404   13.   S. Golunski, *Energ Environ Sci*, 2010, **3**, 1918-1923.
405   14.   S. R. Gomes, N. Bion, G. Blanchard, S. Rousseau, V. Bellière-Baca, V. Harlé, D. Duprez and F.
406   Epron, *Appl Catal B-Environ*, 2011, **102**, 44-53.
407   15.   S. R. Gomes, N. Bion, G. Blanchard, S. Rousseau, D. Duprez and F. Epron, *RSC Adv*, 2011, **1**, 109-
408   116.
409   16.   Y. A. Cengel and M. A. Boles, *Thermodynamics: An Engineering Approach*, Mcgraw-Hill, 1998.

410

411